

Numerical Simulation of NACA 0012 Airfoil Operating under Hailstorm Conditions

Dimitra C. Douvi, Eleni C. Douvi, Dionysios K. Plessas, Dionissios P. Margaritis

Abstract—The current paper refers to the computational study of the aerodynamic behavior of NACA 0012 airfoil operating at Reynolds numbers of $Re=1 \times 10^6$ and $Re=1.76 \times 10^6$ during a hailstorm. The numerical simulations were succeeded using a commercial Computational Fluid Dynamics (CFD) Code in air phase flow as well as in hailstorm conditions, at various angles of attack on the realizable $k-\epsilon$ turbulence model, which cooperates well with the Discrete Phase Model (DPM) by the help of which is succeeded the injection of raindrops and hailstones. The obtained numerical values of the aerodynamic coefficients were validated by comparing them with reliable experimental data, and it was found that hailstorm has negative impact on the aerodynamic performance of the airfoil. Next, the region around the airfoil was studied using contours of static pressure and contours of the concentration of raindrops and hailstones around the airfoil, and the wall film height on the surface of the airfoil is shown.

Index Terms—aerodynamic performance, airfoil, CFD code, hailstorm.

I. INTRODUCTION

Airfoils are extensively used in the construction of wind turbine blades. Since wind turbines operate in open atmosphere, they are exposed to various weather conditions for long time, and their aerodynamic performance can be significantly affected, and the surface of the blades is possible to be eroded too. Recent studies have shown that the annual energy production (AEP) of wind turbines can be considerably affected due to the erosion of blades [1]-[4], the process of which has been computationally examined [5]-[7]. Several authors [8]-[11] also studied the effects of leading-edge roughness on the aerodynamic performance of an airfoil and showed that there is a degradation of the aerodynamic performance.

Next, the aerodynamic behavior of an airfoil operating in multiphase flow has been gaining importance in recent years, because of the growth of Computational Fluid Dynamics (CFD). Several publications have appeared documenting the negative impact of heavy rain on the aerodynamic performance of airfoils by the help of Discrete Phase Model (DPM) [12]-[14]. It was also proven that the wall-film formed on the surface of an airfoil increases the roughness resulting in aerodynamic performance degradation [15],[16].

Dimitra C. Douvi, Mechanical Engineering and Aeronautics Department, University of Patras, Patras, Greece

Eleni C. Douvi, Mechanical Engineering and Aeronautics Department, University of Patras, Patras, Greece

Dionysios K. Plessas, Patras, Greece

Dionissios P. Margaritis, Mechanical Engineering and Aeronautics Department, University of Patras, Patras, Greece

Although many rainstorm conditions have been studied so far over an airfoil, there is still lack in the literature of research on the aerodynamic behavior of an airfoil operating under hailstorm conditions. However, there has been developed a model that simulates numerically the hailstone impacts on aircraft structures and wind turbines [17], and the damaging effects of hailstones on the surface of a blade are examined in detail [18],[19].

The present study concentrates on the aerodynamic behavior of NACA 0012 airfoil operating in hailstorm at two different Reynolds numbers using a commercial CFD code. The computational method and the calculations were also used in previous study [20] that refers to a different airfoil. The validation of the computational results was succeeded by comparing one-phase air flow results with existing reliable experimental data and it was shown that hailstorm conditions have a significant impact on the aerodynamic performance of the airfoil.

II. HAILSTORM CONDITIONS OVER AN AIRFOIL

Hailstorm conditions can be described as a discrete phase flow, which is simulated by the Euler-Lagrange approach. The dispersed phases, in other words the hailstones and the raindrops, interact with the continuum air phase, which means that energy, mass, and momentum of the hailstones and the raindrops are exchanged with the air. Particularly, only momentum is transferred from the air to the dispersed phases as regards hailstorm conditions.

In case an airfoil operates during a hailstorm, the aerodynamic performance of the airfoil is degraded. Specifically, the pressure gradient, the boundary layer, and the shear stress factor can be affected by the presence of hailstones and raindrops. As a result, the lift force decreases while the drag force increases, because of the change in momentum due to the wall-film and the particles that reflect on the airfoil surface.

III. COMPUTATIONAL METHOD

Before the computational study, the geometry of the symmetrical NACA 0012 airfoil was designed in the geometry system, and following a structured C-mesh domain consisted of 80,000 quadrilateral cells was created around the airfoil in mesh component system after a grid independence study conduction [21].

As regards the numerical simulations, they were accomplished by the help of the commercial CFD Code ANSYS Fluent 16 [22], that solves conservation equations for mass, momentum, and supplementary transport equations for turbulent flows. Hailstorm conditions around the airfoil were accomplished by the help of the Lagrangian Discrete

Phase Model (DPM); the Navier-Stokes equations solve the continuum air phase, while many spherical raindrops and hailstones with a diameter of 5 mm are tracked into the calculated flow field. The flow is considered as incompressible, the free stream temperature is set to be 300K, the viscosity and the density of the air are 1.7894×10^{-5} kg/ms and 1.225 kg/m^3 respectively. The mean water content for the hailstones is equal to 1.24 g/m^3 and for the raindrops 2.16 g/m^3 , while the density of hail is set to be 900 kg/m^3 [23].

Next, the dispersed phases are tracked at the minimum distance upstream of the airfoil where the flow is undisturbed to decrease computational time and simplify the solution. The vertical axis velocity of raindrops is calculated by the Markowitz equation [24] and this of hailstones is given by Douglas equation [25], while the horizontal axis velocity of all the particles is equal to air velocity.

The simulations were conducted at Reynolds numbers of $Re=1 \times 10^6$ and $Re=1.76 \times 10^6$ for various angles of attack ranging from -9 to 16 degrees. The flow is turbulent, so the realizable $k-\epsilon$ turbulence model, which was suggested by Shih et al. [26], was chosen for the simulations, since it is appropriate for aerodynamic applications and it cooperates well with Discrete Phase Model (DPM). Raindrops and hailstones damp and product turbulence eddies, that are included in the calculations by enabling two-way turbulence coupling.

Firstly, the steady one-phase air flow around the airfoil was studied and compared to reliable experimental data by Sheldahl and Klimas [27], in order to be validated, and then the study of the steady discrete multiphase flow was conducted via the DPM. The obtained multiphase flow results were compared to the air flow results in order to show the aerodynamic degradation of the airfoil operating under hailstorm conditions.

IV. RESULTS AND DISCUSSION

A. Aerodynamic Coefficients

The aerodynamic lift and drag coefficients were calculated by the help of realizable $k-\epsilon$ turbulence model, and then they were compared with reliable experimental data [27] concerning one-phase air flow over NACA 0012 airfoil.

First of all, Table I presents the numerical values of the lift coefficient versus the angle of attack at $Re=1 \times 10^6$ for air flow and hailstorm conditions. These values are shown graphically in Fig. 1.

Table I. Experimental and numerical data of lift coefficient for NACA 0012 airfoil for Realizable $k-\epsilon$ turbulence model at $Re=1 \times 10^6$ for air flow and hailstorm conditions.

angle of attack	Sheldahl, Klimas (air flow)	Realizable $k-\epsilon$ (air flow)	Realizable $k-\epsilon$ (hailstorm)
-9°	-0.9661	-0.9387	-0.9402
-5°	-0.5500	-0.5319	-0.5351
-3°	-0.3300	-0.3206	-0.3247
0°	0.0000	0.0000	-0.0058
3°	0.3300	0.3206	0.3132
5°	0.5500	0.5320	0.5232
9°	0.9661	0.9387	0.9243
12°	1.1212	1.2127	1.2014
14°	0.8846	1.3662	1.3576

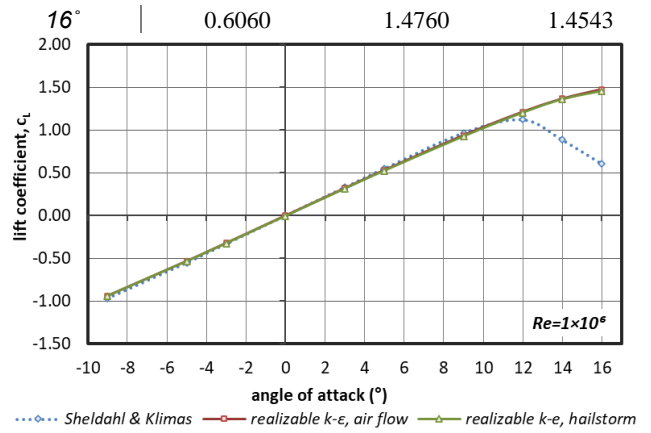


Fig. 1. Comparison between experimental and computational data of the lift coefficient for NACA 0012 airfoil for realizable $k-\epsilon$ turbulence model at $Re=1 \times 10^6$ for air flow and hailstorm conditions.

The air flow numerical values are in good agreement with the corresponding experimental data for small angles of attack, while there is a difference between computational results and experimental data for angles of attack higher than 14 degrees, due to stall conditions. Moreover, the impact of hailstones and water droplets is obvious for all the angles of attack studied. The degradation of lift coefficient reaches a maximum value of -2.29% at angle of attack equal to 3 degrees.

Next, in Table II and Fig. 2 are displayed the experimental and the computational results of the lift coefficient for NACA 0012 airfoil concerning the one-phase air flow, but also the computational results concerning the air-water-hailstones three-phase flow at a Reynolds number of $Re=1.76 \times 10^6$.

In Fig. 2 it can be concluded that the computational values of the lift coefficient behave in accordance with the experimental values for the whole range of possible angles of attack. Furthermore, the lift coefficient curve seems to be slightly downward shifted in hailstorm conditions. The maximum reduction is located at the angle of attack of 3° and it equals with -1.42%.

The above results indicate that as the air velocity increases, the negative effect of the hailstorm on the aerodynamic lift coefficient for NACA 0012 airfoil diminishes.

Table II. Experimental and numerical data of lift coefficient for NACA 0012 airfoil for Realizable $k-\epsilon$ turbulence model at $Re=1.76 \times 10^6$ for air flow and hailstorm conditions.

angle of attack	Sheldahl, Klimas (air flow)	Realizable $k-\epsilon$ (air flow)	Realizable $k-\epsilon$ (hailstorm)
-9°	-0.9138	-0.9497	-0.9494
-5°	-0.5281	-0.5373	-0.5394
-3°	-0.2993	-0.3236	-0.3264
0°	0.0007	0.0000	-0.0037
3°	0.3008	0.3236	0.3190
5°	0.5151	0.5374	0.5313
9°	0.9439	0.9495	0.9374
12°	1.1865	1.2310	1.2268
14°	1.3005	1.3934	1.3885
16°	-	1.5209	1.5058

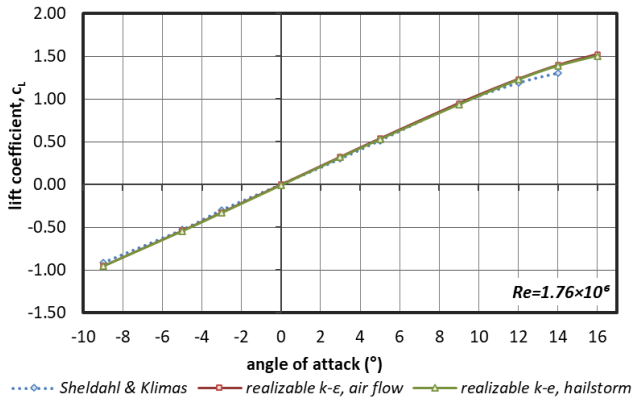


Fig. 2. Comparison between experimental and computational data of the lift coefficient for NACA 0012 airfoil for realizable k-ε turbulence model at $Re=1.76 \times 10^6$ for air flow and hailstorm conditions.

Table III. Experimental and numerical data of drag coefficient for NACA 0012 airfoil for Realizable k-ε turbulence model at $Re=1 \times 10^6$ for air flow and hailstorm conditions.

angle of attack	Sheldahl, Klimas (air flow)	Realizable k-ε (air flow)	Realizable k-ε (hailstorm)
-9°	0.0134	0.0196	0.0195
-5°	0.0091	0.0145	0.0143
-3°	0.0071	0.0132	0.0150
0°	0.0065	0.0125	0.0125
3°	0.0071	0.0132	0.0133
5°	0.0091	0.0145	0.0148
9°	0.0134	0.0196	0.0205
12°	0.0180	0.0269	0.0279
14°	0.0222	0.0345	0.0353
16°	0.1280	0.0458	0.0479

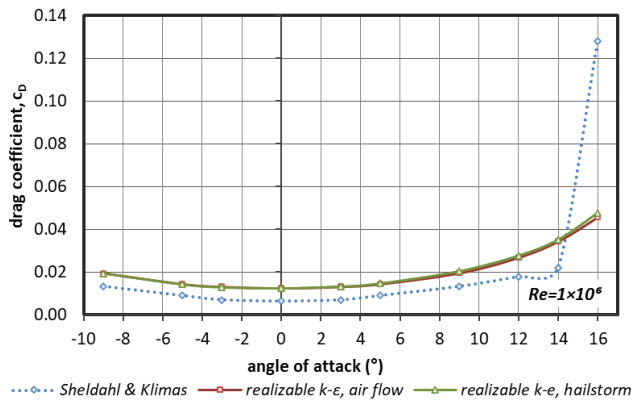


Fig. 3. Comparison between experimental and computational data of the drag coefficient for NACA 0012 airfoil for realizable k-ε turbulence model at $Re=1 \times 10^6$ for air flow and hailstorm conditions.

Following, Table III shows the computational results of the drag coefficient of NACA 0012 airfoil, when the airfoil operates in air flow as well as under hailstorm conditions, at a Reynolds number of $Re=1 \times 10^6$. As it can be seen in Fig. 3, the numerical values of the drag coefficient are greater than the corresponding experimental for angles of attack ranging between -9° and 14° , due to the incapability of the turbulence model to accurately compute the transition point of the boundary layer from laminar to turbulent, but at 16° the

computational value is lower. The impact of the hailstorm conditions on the drag coefficient is obvious, since the values of drag coefficient are increased in multiphase flow. More specifically, at positive angles of attack the drag coefficient values in hailstorm are greater than the corresponding values in air flow. As the angle of attack increases, the impact of multiphase flow on the aerodynamic drag coefficient gets more intense. The maximum increase of the coefficient is at the angle of 9° and is equal to 4.66%.

Subsequently, Table IV and Fig. 4 depict the experimental results of the drag coefficient versus the angle of attack in air flow at $Re=1.76 \times 10^6$, and the corresponding values that emerged computationally for air flow and hailstorm conditions. It is shown that the experimental values of the drag coefficient are lower than the predicted values for a wide range of angles of attack. Also, as the angle of attack increases, the difference between experimental and numerical curves is getting greater, and under hailstorm conditions there is an upward translation of the drag coefficient curve because of the larger skin frictional drag caused by the presence of raindrops and hailstones. The maximum increase of the drag coefficient is shown at 16° and is equal to 7.71%.

Finally, it can be concluded that the aerodynamic drag coefficient is negatively affected under hailstorm conditions, since higher values are achieved and especially at higher angles of attack.

Table IV. Experimental and numerical data of drag coefficient for NACA 0012 airfoil for Realizable k-ε turbulence model at $Re=1.76 \times 10^6$ for air flow and hailstorm conditions.

angle of attack	Sheldahl, Klimas (air flow)	Realizable k-ε (air flow)	Realizable k-ε (hailstorm)
-9°	0.0167	0.0179	0.0179
-5°	0.0101	0.0132	0.0131
-3°	0.0079	0.0120	0.0119
0°	0.0061	0.0113	0.0114
3°	0.0061	0.0120	0.0121
5°	0.0071	0.0132	0.0133
9°	0.0117	0.0180	0.0188
12°	0.0159	0.0246	0.0253
14°	0.0183	0.0314	0.0325
16°	-	0.0410	0.0442

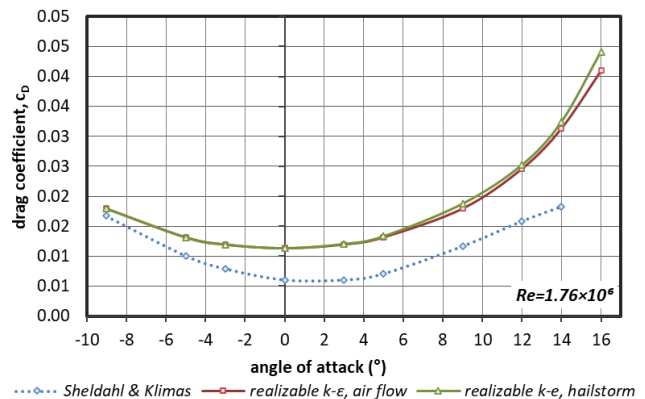


Fig. 4. Comparison between experimental and computational data of the drag coefficient for NACA 0012 airfoil for realizable k-ε turbulence model at $Re=1.76 \times 10^6$ for air flow and hailstorm conditions.

B. Contours of Static Pressure

Next, from Fig. 5 to Fig. 8 are given the contours of static pressure around NACA 0012 airfoil that operates in air flow and during hailstorm at angles of attack equal to -5° and 3° and at two different Reynolds numbers, as emerged by the help of realizable $k-\epsilon$ turbulence model. To start with, Fig. 5 illustrates the contours of static pressure around NACA 0012 airfoil operating in air flow for -5° and 3° angles of attack at the Reynolds number of $Re=1 \times 10^6$. The stagnation points, where static pressure is equal to total, are obvious at both angles of attack. It is observed that at the negative angle of attack stagnation point is on the upper surface of the airfoil, while for the positive angle of attack it is on the lower surface close to the leading edge of the airfoil. Also, it is shown that the values of static pressure are higher on the upper surface of the airfoil for the negative angle of attack, and higher on the lower surface at the angle of attack equal to 3° . Moreover, static pressure seems to be increased in the region of the trailing-edge of the airfoil.

Fig. 6 depicts the contours of static pressure around the airfoil operating under hailstorm conditions for the same angles of attack. It should be noticed that there are minor differences between contours in Fig. 5 and in Fig. 6 mainly on the lower surface of the airfoil as well as in the region near the trailing-edge. In general, the aerodynamic behavior of the airfoil remains the same for each angle of attack.

Similarly, Fig. 7 and Fig. 8 show the contours of static pressure around the airfoil at the same angles of attack at $Re=1.76 \times 10^6$ for air flow and hailstorm conditions. The emerged results are similar to those obtained for $Re=1 \times 10^6$, but as the air velocity increases, static pressure values get greater.

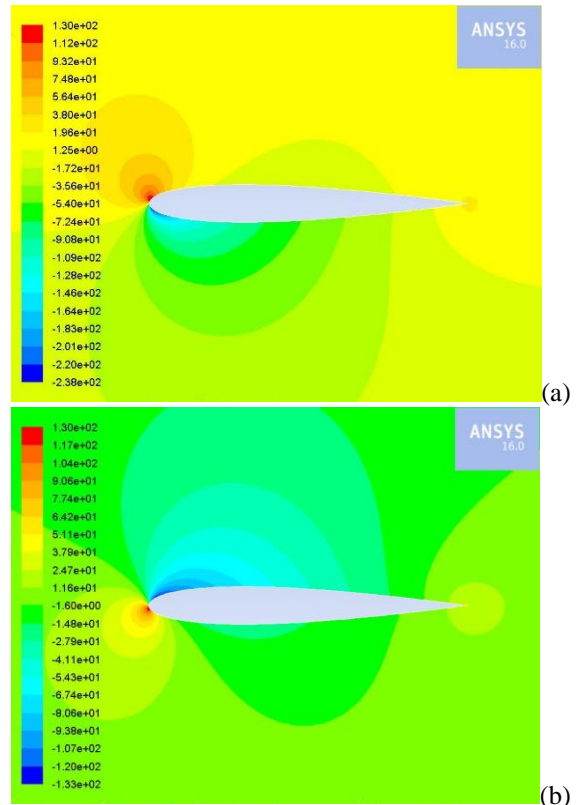


Fig. 5. Contours of static pressure [Pa] at (a) -5° and (b) 3° angles of attack at $Re=1 \times 10^6$ with the realizable $k-\epsilon$ turbulence model for NACA 0012 airfoil in air flow.

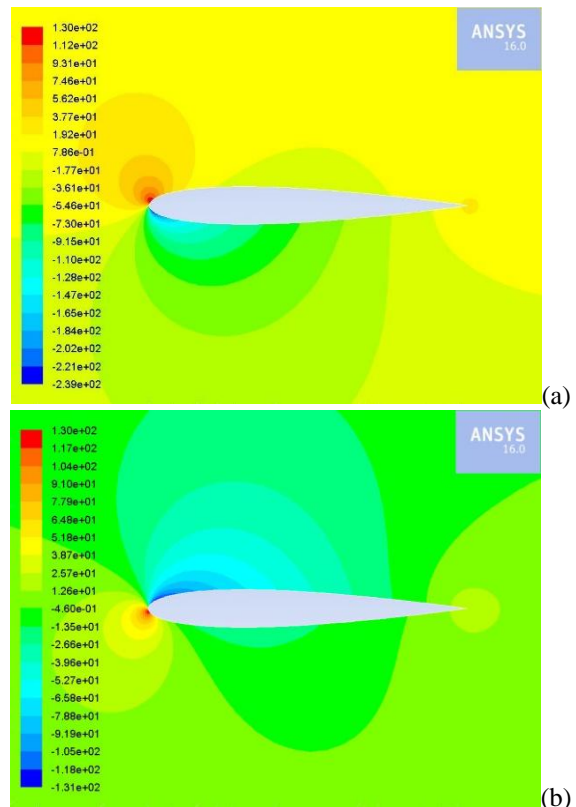


Fig. 6. Contours of static pressure [Pa] at (a) -5° and (b) 3° angles of attack at $Re=1 \times 10^6$ with the realizable $k-\epsilon$ turbulence model for NACA 0012 airfoil in hailstorm conditions.

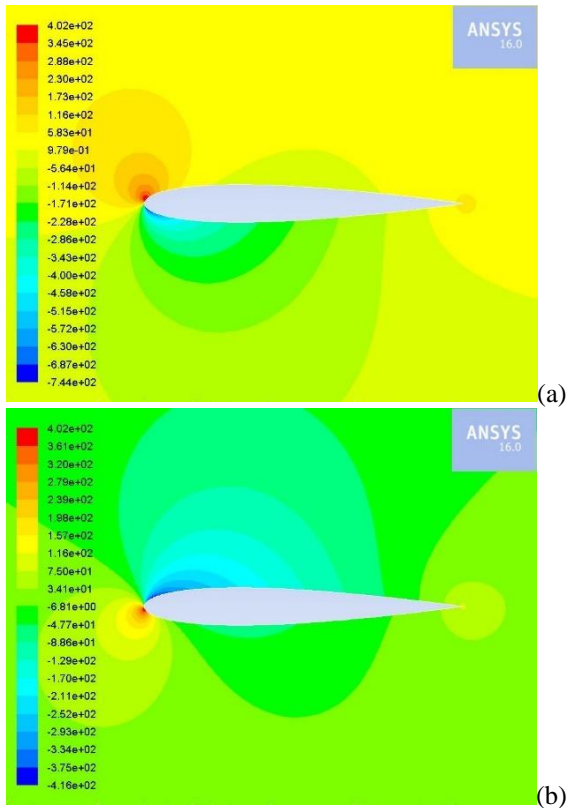


Fig. 7. Contours of static pressure [Pa] at (a) -5° and (b) 3° angles of attack at $Re=1.76 \times 10^6$ with the realizable $k-\epsilon$ turbulence model for NACA 0012 airfoil in air flow.

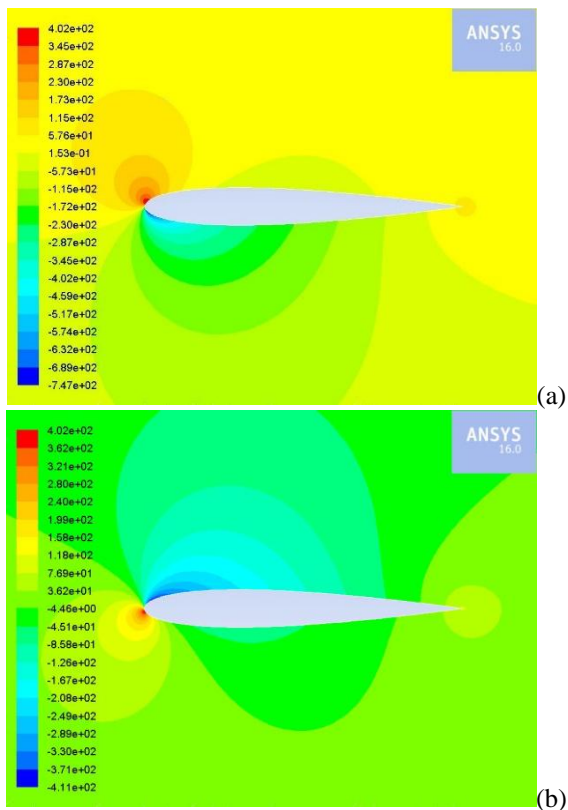


Fig. 8. Contours of static pressure [Pa] at (a) -5° and (b) 3° angles of attack at $Re=1.76 \times 10^6$ with the realizable $k-\epsilon$ turbulence model for NACA 0012 airfoil in hailstorm conditions.

C. Concentration of particles and water film height

Fig. 9 and Fig. 10 present the concentration of raindrops and hailstones on the surface of the airfoil with the realizable $k-\epsilon$ turbulence model. It is shown that the concentration of the dispersed phases particles is greater at the leading edge and mostly on the upper surface of the airfoil for all the angles of attack and at both Reynolds numbers. Furthermore, it is observed that as the Reynolds number increases, more raindrops and hailstones concentrate near the leading edge of the airfoil, but at the same time the region occupied by the particles on the upper surface of the airfoil is smaller, because particles are drifted away more easily by the air.

Next, Fig. 11 and Fig. 12 show the height of the water-film created on the surface of NACA 0012 airfoil operating during hailstorm for two different Reynolds numbers. It seems that water-film is formed mostly on the upper surface of the airfoil, and in the areas of the upper and lower surfaces close to the leading edge. The height of water-film varies on the upper surface. More specifically, the film is thicker near the leading edge, but it fluctuates on the other areas of the upper surface up to the trailing-edge. In the region around the trailing-edge of the airfoil can be seen the paths followed by raindrops and hailstones, and it is shown that their direction changes with angle of attack. Furthermore, as the air velocity increases, it seems that there are fewer areas on the upper surface of the airfoil where water-film is high. Simultaneously, the maximum height of the water-film near the leading-edge increases since particles impact the airfoil with greater velocity.

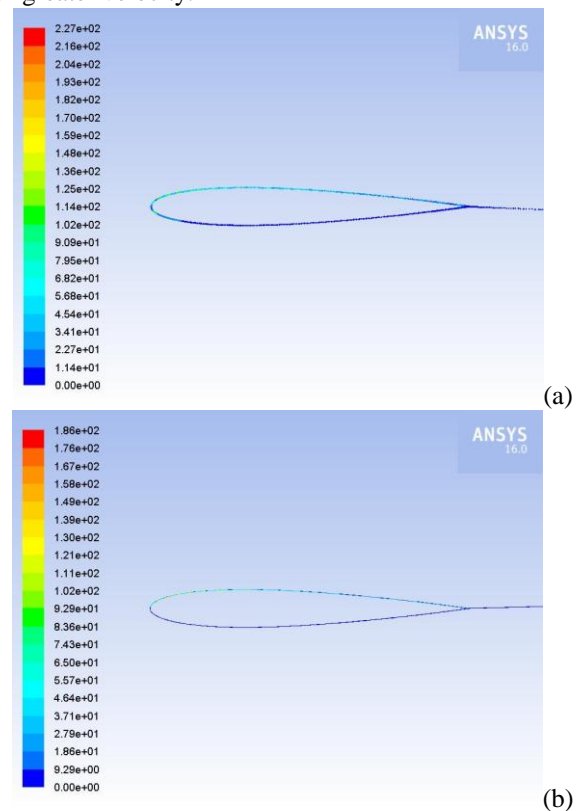


Fig. 9. Concentration of raindrops and hailstones around NACA 0012 airfoil at (a) -5° and (b) 3° angle of attack at $Re=1 \times 10^6$ with the realizable $k-\epsilon$ turbulence model for hailstorm conditions.

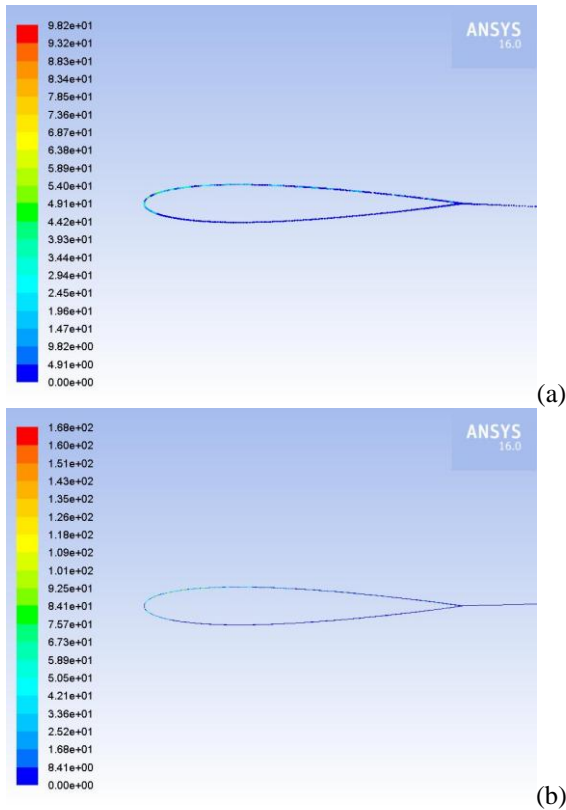


Fig. 10. Concentration of raindrops and hailstones around NACA 0012 airfoil at (a) -5° and (b) 3° angle of attack at $Re=1.76 \times 10^6$ with the realizable $k-\epsilon$ turbulence model for hailstorm conditions.

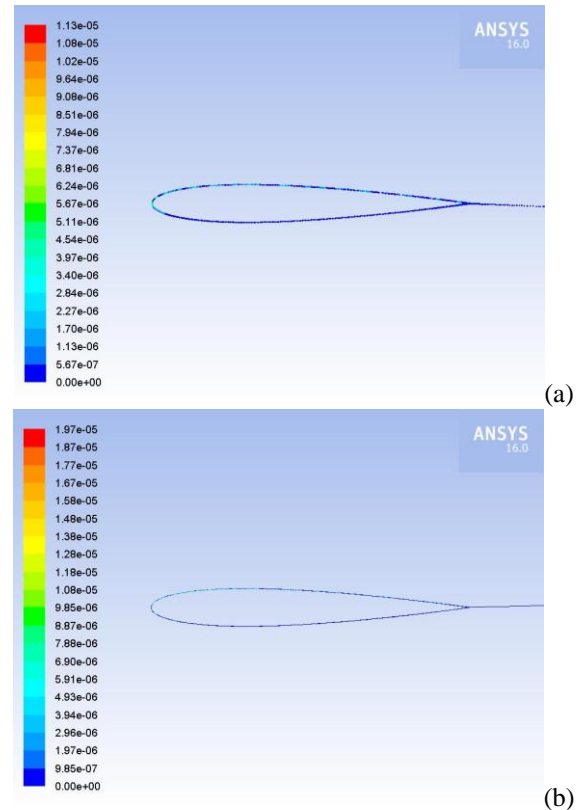


Fig. 12. Water-film height [m] around NACA 0012 airfoil at (a) -5° and (b) 3° angle of attack at $Re=1.76 \times 10^6$ with the realizable $k-\epsilon$ turbulence model for hailstorm conditions.

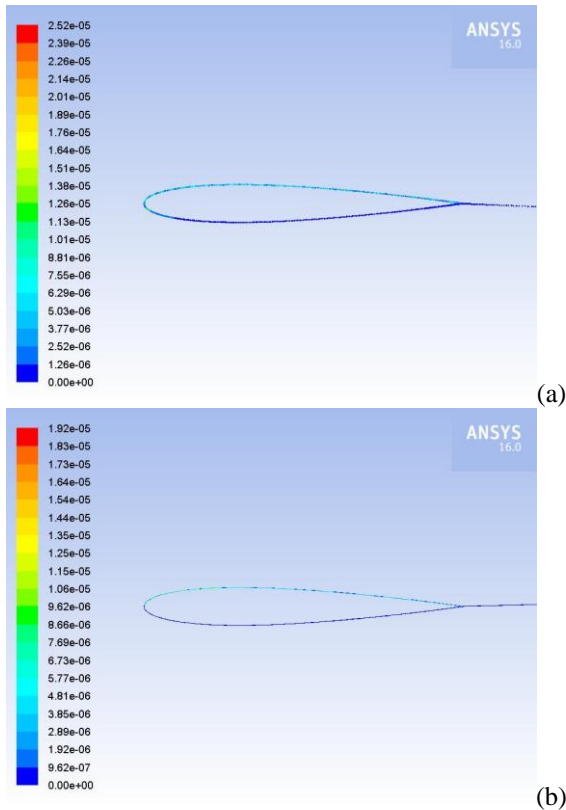


Fig. 11. Water-film height [m] around NACA 0012 airfoil at (a) -5° and (b) 3° angle of attack at $Re=1 \times 10^6$ with the realizable $k-\epsilon$ turbulence model for hailstorm conditions.

V. CONCLUSION

The present study concentrates computationally on the aerodynamic behavior of NACA 0012 airfoil operating at Reynolds numbers of $Re=1 \times 10^6$ and $Re=1.76 \times 10^6$ during a hailstorm by the help of realizable $k-\epsilon$ turbulence model, and it has can be concluded that air-water-hailstones multiphase flow has a negative effect on the aerodynamic performance of the airfoil.

More specifically, by the computational study it was shown that lift coefficient values reduce and drag coefficient values increase for a wide range of angles of attack due to hailstorm conditions in comparison with the corresponding coefficient values in one-phase air flow. Also, it was found that as the angle of attack increases the impact of hailstorm on lift coefficient diminishes, while drag coefficient gets higher. As regards the air velocity, it can be concluded that as Reynolds number increases, the effect of multiphase flow on lift coefficient is less intense.

Following, contours of static pressure around the airfoil indicate that as air velocity increases, the behavior of the airfoil is similar at each angle of attack, but static pressure values get greater. It is also suggested that static pressure is greater on the lower surface of the airfoil at positive angles of attack and higher on the upper surface at negative angles of attack. Furthermore, the stagnation points are detected close to the leading edge of the airfoil, and static pressure seems to be higher in the region of the trailing-edge. Under hailstorm conditions it was shown that the aerodynamic behavior of the airfoil remains almost the same, since there are minor differences mainly close to the trailing edge as well as on the

lower and on the upper surface of the airfoil, where static pressure gets higher and lower respectively.

Based on the presentation of the concentration of raindrops and hailstones on the surface of the airfoil, it can be concluded that the dispersed phases particles concentrate more at the leading edge and on the upper surface of the airfoil. As the flow velocity increases, the number of particles on the surface is greater, but at the same time less space on the upper surface of the airfoil is occupied by them. Next, it was concluded that the formed water-film is thicker close the leading edge, while its height fluctuates on the upper surface up to the trailing edge. In addition, as air velocity increases, there are fewer regions on the upper surface where water-film is high, but the maximum height of the film near the leading-edge increases.

REFERENCES

[1] F. Papi, F. Balduzzi, G. Ferrara, and A. Bianchini, "Uncertainty quantification on the effects of rain-induced erosion on annual energy production and performance of a Multi-MW wind turbine," *J. Renewable Energy*, vol. 165, Nov. 2020, pp. 701-715 Available: <https://doi.org/10.1016/j.renene.2020.11.071>.

[2] W. Han, J. Kim, and B. Kim, "Effects of contamination and erosion at the leading edge of blade tip airfoils on the annual energy production of wind turbines," *J. Renewable Energy*, vol. 115, Jan. 2018, pp. 817-823 Available: <https://doi.org/10.1016/j.renene.2017.09.002>.

[3] M. Schramm, H. Rahimi, B. Stoevesandt, and K. Tangager, "The influence of eroded blades on wind turbine performance using numerical simulations", *J. Energies*, vol. 10(9), Sept. 2017 Available: <https://doi.org/10.3390/en10091420>.

[4] A. Sareen, C. A. Sapre, and M. S. Selig, "Effects of leading-edge erosion on wind turbine blade performance," *J. Wind Energy*, vol. 17, Oct. 2014, pp. 1531–1542 Available: <https://doi.org/10.1002/we.1649>.

[5] Y. Wang, R. Hu, and X. Zheng, "Aerodynamic Analysis of an Airfoil with Leading Edge Pitting Erosion," *J. Solar Energy Engineering*, Transactions of the ASME, vol. 139(6), Dec. 2017 Available: <https://doi.org/10.1115/1.4037380>.

[6] Y. Wang, R. Hu, and P. Wang, "Research on the aerodynamic and flow field characteristics of S809 airfoil based on the leading-edge erosion modeling," *J. Taiyangneng Xuebao/Acta Energiae Solaris Sinica*, vol. 38(3), Mar. 2017, pp. 607-615.

[7] D. Li, C. Wang, Y. Li, R. Li, Z. Zhao, and X. Chen, "Influence of blade leading edge erosion features on aerodynamic characteristics of wind turbine airfoil," *J. Transactions of the Chinese Society of Agricultural Engineering*, vol. 33(22), Nov. 2017, pp. 269-275.

[8] J. M. Janiszewska, R. Reuss Ramsay, M. J. Hoffmann, and G. M. Gregorek, *Effects of Grit Roughness and Pitch Oscillations on the S814 Airfoil*, Technical Report, NREL/TP-442-8161, National Renewable Energy Laboratory, Golden, CO, USA, 1996 Available: <https://doi.org/10.2172/273772>.

[9] O. Pires, X. Munduate, K. Boorsma, O. Ceyhan Yilmaz, H. Aa Madsen, and W.A. Timmer, (2018), "Experimental investigation of Surface Roughness effects and Transition on Wind Turbine performance," *J. Physics: Conference Series*, vol. 1037(5), Jun. 2018, Available: <https://doi.org/10.1088/1742-6596/1037/5/052018>.

[10] Y. Zhang, "Effects of distributed leading-edge roughness on aerodynamic performance of a low-Reynolds-number airfoil: an experimental study," *J. Theoretical and Applied Mechanics Letters*, vol. 8(3), May 2018, pp. 201-207 Available: <https://doi.org/10.1016/j.taml.2018.03.010>.

[11] I. Zidane, K. Saqr, G. Swadener, X. Ma, and M. Shehadeh (2016), "On the role of surface roughness in the aerodynamic performance and energy conversion of horizontal wind turbine blades: A review", *International J. Energy Research*, vol. 40(15), Jun. 2018, pp. 2054-2077 Available: <https://doi.org/10.1002/er.3580>.

[12] E. C. Douvi, and D. P. Margaris, "Aerodynamic performance investigation under the influence of heavy rain of a NACA 0012 airfoil for wind turbine applications," *J. International Review of Mechanical Engineering (IREME)*, vol. 6(6), Sep. 2012, pp. 1228–1235

[13] T. Wan, and C. J. Chou, "Reinvestigation of high lift airfoil under the influence of heavy rain effects," *50th AIAA Aerospace Sciences Meeting Including the New Horizons Forum and Aerospace*

Exposition, 9–12 Jan. 2012, Nashville, Tennessee Available: <https://doi.org/10.2514/6.2012-1202>.

[14] Z. Wu, and Y. Cao "Numerical simulation of flow over an airfoil in heavy rain via a two-way coupled Eulerian-Lagrangian approach," *Int. J. Multiphase Flow*, vol. 69, Mar. 2015, pp. 81-92 Available: <https://doi.org/10.1016/j.ijmultiphaseflow.2014.11.006>.

[15] E. Hastings, and G. Manuel, "Scale–model tests of airfoils in simulated heavy rain," *J. Aircraft*, vol. 22(6), 1985, pp. 536-540, Available: <https://doi.org/10.2514/3.45161>.

[16] R. Hansman, and M. Barsotti, "The Aerodynamic Effect of Surface Wetting Characteristics on a Laminar Flow Airfoil in Simulated Heavy Rain," AIAA Paper 85-0260, 1985 Available: <https://doi.org/10.2514/6.1985-260>.

[17] M. A. Lavoie, A. Gakwaya, M. J. Richard, M. N. Nandlall, M. N. Ensan, and D. G. Zimcik, "Numerical and experimental modeling for bird and hail impacts on aircraft structure," *IMAC-XXVIII Society for Experimental Mechanics*, Jacksonville, Florida, USA, vol. 3, 1-4 Feb. 2011, pp. 1403-1410 Available: https://doi.org/10.1007/978-1-4419-9834-7_123.

[18] M. H. Keegan, D. Nash, and M. Stack, "Numerical modelling of hailstone impact on the leading edge of a wind turbine blade," *European Wind Energy Conference and Exhibition, EWEC 2013*, Vienna, Austria, 4-7 Feb. 2013, pp. 92-102

[19] G. Fiore, G. E. C. Fujiwara, and M. S. Selig, "A damage assessment for wind turbine blades from heavy atmospheric particles," *53rd AIAA Aerospace Sciences Meeting*, Kissimmee, Florida, USA, 5-9 Jan. 2015.

[20] D. C. Douvi, A.-G. K. Georgakopoulos, D. I. Lekkas, E. C. Douvi, and D. P. Margaris, "Aerodynamic degradation of a three bladed horizontal axis wind turbine operating during a hailstorm," *8th International Conference on "Experiments/ Process/ System Modeling/ Simulation/ Optimization"* (8th IC-EPSMSO), Athens, Greece, 3-6 Jul. 2019.

[21] D. C. Douvi, E. C. Douvi and D. P. Margaris, "Computational study of NACA 0012 airfoil in air-sand particle two-phase flow at Reynolds number of $Re=1.76 \times 10^6$," *Int. J. of New Technology and Research (IJNTR)*, vol. 5(4), Apr. 2019, pp.101-108 Available <https://doi.org/10.31871/IJNTR.5.4.18>

[22] ANSYS® (2019, March 20). Academic Research (Release 16.0) [Online]. Available: <http://www.ansys.com>

[23] B. Federer, and A. Waldvogel, "Hail and Raindrop Size Distributions from a Swiss Multicell Storm," *J. Applied Meteorology*, vol. 14, Feb. 1975, pp. 91-97 Available: [https://doi.org/10.1175/1520-0450\(1975\)014<0091:HARSDF>2.0.CO;2](https://doi.org/10.1175/1520-0450(1975)014<0091:HARSDF>2.0.CO;2).

[24] A. Markowitz, "Raindrop Size Distribution Expression," *J. Applied Meteorology*, vol. 15, 1976, pp. 1029-1031.

[25] R. H. Douglas, "Hail size distributions", *International Conference on Radiometeorology, 11th Weather Radar*, Boulder, Colorado, 14-18 Sep. 1964, pp. 146-149.

[26] T.-H. Shih, W. W. Liou, A. Shabbir, Z. Yang, and J. Zhu, "A new k-ε eddy-viscosity model for high Reynolds number turbulent flows—model development and validation," *J. Computers Fluids*, vol.24(3), Mar. 1995, pp. 227–238. Available: [https://doi.org/10.1016/0045-7930\(94\)00032-T](https://doi.org/10.1016/0045-7930(94)00032-T).

[27] R. Sheldahl and P. Klimas, *Aerodynamic characteristics of seven airfoil sections through 180 degrees angle of attack for use in aerodynamic analysis of vertical axis wind turbines*, Sandia National Laboratories, New Mexico, 1981.



Dimitra C. Douvi, born in Korinthos, Greece on May 31st, 1989. She has Ph.D. in Mechanical Engineering and Aeronautics Department and B.Sc. in Mathematics Department of the University of Patras. Her doctoral thesis is experimental and computational investigation of aerodynamic behavior of wind turbine rotor in multiphase flows. Her research activities/fields are multiphase flows, wind energy systems, computational fluid dynamics, aerodynamics, development of computational codes. She is participating in 7 international conferences on the above scientific areas and has 4 publications on high-interested impact factor Journals. Dr. Dimitra Douvi is participating in 2 research projects supported by BIG SOLAR S.A. in Greece.



Eleni C. Douvi, born in Korinthos, Greece on March 15th, 1984. She is post-doctoral researcher of Mechanical Engineering and Aeronautics Department at University of Patras. Her research activity as post-doctoral researcher is CFD analysis of innovative solar collector with integration of Phase Change Materials, as well as the proposal of the optimum geometry of a horizontal axis tidal turbine rotor. Her

doctoral thesis was experimental and computational investigation of aerodynamic behavior of wings in heavy rain, applied to horizontal axis wind turbine blades. In her diploma thesis was dealing with the experimental study of fluid mechanics applying LDA and PDA measurements. Her research activities/fields are wind and solar energy systems, tidal turbines, multiphase flows, computational and experimental fluid dynamics, aerodynamics, hydrodynamics, phase change materials, heat transfer and development of computational codes. She is participating in 14 international conferences on the above scientific areas and has 10 publications on high-interested impact factor Journals. She has been awarded an Heracleitus II PhD Fellowship for her doctoral thesis and a scholarship from Greek State Scholarships Foundation (IKY) for postdoctoral research in Greece. Dr. Eleni Douvi is participating in several research projects funding by General Secretariat for Research and Technology and BIG SOLAR S.A. Also she is member of TCG (Technical Chamber of Greece).



Dionysios K. Plessas, born in Patras, Greece on November 19th, 1988. He has B.Sc. in Physics Department of the University of Patras. His research activities/fields are multiphase flows, computational fluid dynamics, aerodynamics, development of computational codes, computational astrophysics, electronics and digital signal processing, applied acoustics.



Dionissios P. Margaris, born in Zakynthos island, Greece on September 28th, 1953. He is Professor in Mechanical Engineering and Aeronautics Department at the University of Patras, Patras, Greece. His research activities/fields are multiphase flows of gas-liquid-solid particles, gas-liquid two-phase flow air-lift pump performance, centrifugal and T-junction separation modeling in gas-liquid two-phase flow, experimental and theoretical investigation of hot air dehydration of agricultural products, experimental and theoretical investigation of capillary pumped loops, steady and transient flows in pipes and network and numerical simulation of centrifugal pump performance. Also he is dealing with fluid dynamics analysis of wind turbines and aerodynamic installations, aero-acoustic analysis and environmental impacts of wind turbines. He is participating in over 130 international conferences on the above scientific areas and has over 80 publications on high-interested impact factor Journals. Prof. Dionissios P. Margaris is participating in several research projects supported by HAI, GSRT, CEC-THERMIE. Also he is member of AIAA, AHS, ASME and EUROMECH unions as well as of TCG (Technical Chamber of Greece).